Journal of Organometallic Chemistry 693 (2008) 3233–3239

Contents lists available at ScienceDirect

Journal of Organometallic Chemistry

journal homepage: www.elsevier.com/locate/jorganchem

Synthesis of *E*-alkenylsilanes with dithienosilole and their electrochemical and optical properties

In-Sook Lee [a], Young-Woo Kwak [a,*], Dong-Ha Kim [a], Yong Cho [b], Joji Ohshita [c]

[a] Department of Chemistry, Kyungpook National University, Daegu 702-701, Republic of Korea
[b] R&D Center, Heesung Electronics Ltd., Hosan-Dong, Dalseo-Gu, Daegu 704-230, Republic of Korea
[c] Department of Applied Chemistry, Graduate School of Engineering, Hiroshima University, Higashi-Hiroshima 739-8527, Japan

ARTICLE INFO

Article history:
Received 7 September 2007
Received in revised form 4 July 2008
Accepted 4 July 2008
Available online 31 July 2008

Keywords:
Hydrosilylation
Silylene-spacer
4,4-Diphenyldithienosilole
Alkenylsilane
Quantum yield

ABSTRACT

A series of 2,6-bis(ethenylsilyl)-4,4-diphenyldithienosilole derivatives containing silylene-spacer were prepared by platinum-catalyzed hydrosilylation reaction. All the hydrosilylation proceeded regio- and stereoselectively to give solely β-(*E*)-adducts. The 2,6-bis(ethenylsilyl)-4,4-diphenyldithienosilole derivatives exhibit intense fluorescence emission and high quantum yields. The shoulder band of **9** in the emission spectrum was explained the intramolecular charge transfer from the electron-donating group (dimethylaminostyryl group) to electron-accepting group (dithienosilole moiety). These optical data are in good agreement with the results of theoretical calculations of model compounds at the level of B3LYP/6-31G(d,p).

1. Introduction

Many papers concerning the transition metal-catalyzed hydrosilylation of carbon–carbon unsaturated molecules, which is an important process generating alkenylsilanes, have been published to date [1]. The organic materials possessing alternative arrangement of an organosilicon and π-electron system in their backbone are of current interest, because they can be used as functionality materials such as carrier transporting materials and emissive materials [2]. It has recently been reported that introduction of silylene moiety into a π-electron system of some organic semiconductors and hole transporting materials enhances luminescence properties [3]. We have reported the synthesis of several σ–π conjugated polymers containing organosilanylene and dithienosilole (DTS) derivatives which could be used as both electron- and hole-transporting layer for the electroluminescence (EL) devices [4]. Furthermore, focus has also been directed towards the synthesis of diverse materials containing DTS moiety for electroluminescent device applications due to its low-lying LUMO level [5,6], arising from the interaction between the silicon σ^* and butadiene π^* orbitals. Therefore, dithienosilole became our backbone of choice. Introduction of a flexible spacer such as $SiMe_2$ into the well-defined chromophore of dithienosilole [3] or diphenylanthracene [7] unit is current topic in luminescent materials. To our knowledge, introduction of silylene-spacer into the monomeric dithienosilole derivatives has not reported yet. We have designed the synthesis of new alkenylsilanes with dithienosilole moiety by adopting platinum-catalyzed hydrosilylation. Described herein are the synthesis, optical, and electrochemical properties of novel silylene-spaced dithienosilole derivatives (**3**–**10**) by hydrosilylation of 2,6-bis(dimethylsilyl)-4,4-diphenyldithienosilole (**2**) with various terminal alkynes using platinum(0) catalyst.

2. Results and discussion

2.1. Synthesis and characterization

The schematic representation describing the route of synthesis is illustrated in Scheme 1. When 2,6-dilithio-4,4-diphenyldithienosilole, which was prepared from 2,6-dibromo-4,4-diphenyldithienosilole [5] (**1**) using *N*,*N*,*N*′,*N*′-tetramethylethylenediamine (TMEDA) and *n*-butyllithium, was treated with chlorodimethylsilane, a new organosilylene-dithienosilole derivative, 2,6-bis(dimethylsilyl)-4,4-diphenyldithienosilole (BDMS-DTS, **2**) was afforded in 70% yield. When 1 equiv of the BDMS-DTS (**2**) was subjected to the hydrosilylation reaction with 2 equiv of *tert*-butylacetylene in the presence of ethylenebis(triphenylphosphine)-platinum(0) (1 mol%) in hexane at 40 °C for 12 h, 2,6-bis{[(*E*)-2-*tert*-butylethenyl]dimethylsilyl}-4,4-diphenyldithienosilole (**3**) was formed in 89% yield after the purification over silica gel column chromatography. Similarly, a series of 2,6-bis(ethenylsilyl)-4,

* Corresponding author. Tel.: +82 53 950 5339; fax: +82 53 950 6330.
E-mail address: ywkwak@knu.ac.kr (Y.-W. Kwak).

0022-328X/$ - see front matter © 2008 Elsevier B.V. All rights reserved.
doi:10.1016/j.jorganchem.2008.07.030

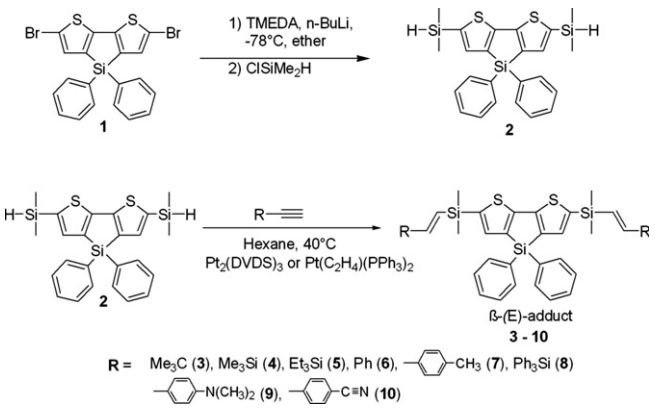

Scheme 1.

4-diphenyldithienosilole derivatives (**4–10**) was synthesized from BDMS-DTS (**2**) by adopting the hydrosilylation reaction with various terminal alkynes in place of *tert*-butylacetylene. The synthesis of all the 2,6-bis(ethenylsilyl)-4,4-diphenyldithienosilole derivatives (**3–10**) was achieved in hexane except **8**, which was achieved in THF due to the poor solubility of the terminal alkyne, triphenylsilylacetylene, in hexane. The yields of their corresponding 2,6-bis(ethenylsilyl)-4,4-diphenyldithienosilole derivatives (**4**, **5**, and **8**) were unsatisfactory when a catalytic amount of ethylenebis(triphenylphosphine)platinum(0) was employed. Therefore, the hydrosilylation reactions of BDMS-DTS (**2**) with the terminal alkynes such as trimethyl-, triethyl-, and triphenylsilylacetylene were carried out in the presence of platinum(0)-1,3-tetramethyldivinyldisiloxane complex $Pt_2(DVDS)_3$ known as Karstedt's catalyst (1 mol%). In all the cases, the temperature of reactions was maintained at 40 °C and the reactions were completed in 12–24 h as evidenced by thin-layer chromatography.

As shown in Table 1, the hydrosilylated adducts (**3–7**) were obtained in good yield, while the adducts **8–10** were moderate. The structures of compounds (**3–10**) were identified through the coupling constant (J) of ^{1}H NMR characteristic signals of vinylic protons showed from 18.9 to 22.6 Hz. For the all products, the hydrosilylation proceeds regio- and stereoselectively to give solely β-(*E*)-products (**3–10**). Characteristic signals of the ^{1}H NMR spectrum at 5.66 and 6.18 (doublet, J = 19.2 Hz, respectively) of **3**, a selection of the hydrosilylated adducts, clearly shows the formation of *E*-alkenylsilane with dithienosilole. The signals of two methyl protons of the $SiMe_2$ group adjacent to the DTS moiety are affected slightly by the R substituents. The ^{29}Si NMR spectrum of **5** exhibits three single resonances at δ −22.05, −15.78, and −1.02 ppm, which are assigned to the silicon atoms of dithienosilole, dimethylsilylene, and trimethylsilyl group, respectively. This result implies that the adduct has the regular structure of dithienosilole and *E*-alkenylsilane units.

2.2. Optical and electrochemical properties of hydrosilylated adducts

The UV absorption and emission spectra of hydrosilylated adducts (**3–10**) were taken in THF solution and are shown in Figs. 1 and 2, respectively.

The λ_{max} values of absorption and emission are listed in Table 2. As a whole, the absorption bands at 357 nm indicate that all the electronic transitions are mostly $\pi \rightarrow \pi^*$, originating from the system of 4,4-diphenyldithienosilole. The absorption bands are little affected by the R substituents on silicon atoms [8] which are connected to the dithienosilole ring. However, the absorption maximum of **9** is slightly red-shifted 5 nm as compared with those of the other hydrosilylated adducts (**3–8** and **10**), which is due to the electron-donating group such as dimethylamino group at *para*-position of phenyl substituent. The emission bands of hydrosilylated adducts (**3–10**) in THF solution appeared between 426 and 429 nm which were red-shifted about 6 nm as compared with that of the reactant (**2**) (Table 2). The σ–π interaction between the Si–C bonding orbital and π^*-orbital of the conjugated chromophore was very weak to be characterized in the hydrosilylated adducts. Accordingly, the dimethylsilylene moiety may be considered essentially as an insulating spacer [7,9]. In comparison

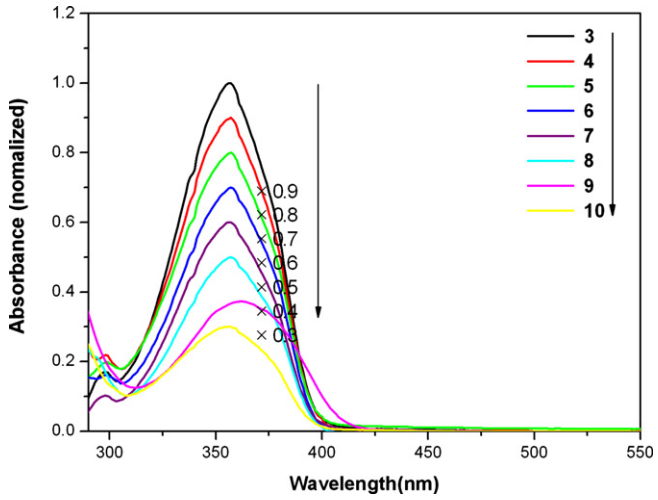

Fig. 1. UV–Vis spectra of the hydrosilylated adducts **(3–10)** in THF with normalized absorbance (the arrow in spectra indicates the order of number of the compounds).

Table 1
Hydrosilylation of terminal alkynes catalyzed by Pt(0) catalysts with **2** and NMR data of the adducts (**3–10**)

Compound	Catalyst[a]	Yield[b] (%)	Mp (°C)	NMR[c] (ppm)		
				^{29}Si	^{1}H	
					$Si(Me)_2$	HC=CH
3	A	88	126–127	−22.03, −14.42	0.38	5.66 (J = 19.2 Hz) 6.18 (J = 19.2 Hz)
4	B	51	144–145	−21.93, −15.62 −7.15	0.39	6.68 (J = 22.6 Hz) 6.76 (J = 22.1 Hz)
5	B	50	94–96	−22.05, −15.78 −1.02	0.39	6.68 (J = 20.6 Hz) 6.74 (J = 20.6 Hz)
6	A	63	135–136	−22.05, −13.86	0.47	6.56 (J = 18.9 Hz) 6.97 (J = 18.9 Hz)
7	A	63	126–128	−22.06, −13.92	0.48	6.52 (J = 19.1 Hz) 6.96 (J = 19.1 Hz)
8	B	37	82–83	−22.11, −17.16 −15.02	0.44	6.92 (J = 22.1 Hz) 7.26 (J = 22.1 Hz)
9	A	38	156–157	−22.09, −14.06	0.46	6.31 (J = 19.0 Hz) 6.91 (J = 19.0 Hz)
10	A	34	125–127	−22.69, −13.52	0.51	6.73 (J = 19.1 Hz) 6.96 (J = 19.1 Hz)

[a] The kinds of catalysts: A, $Pt(C_2H_4)(PPh_3)_2$; B, $Pt_2(DVDS)_3$.
[b] Isolated yields.
[c] TMS reference in $CDCl_3$.

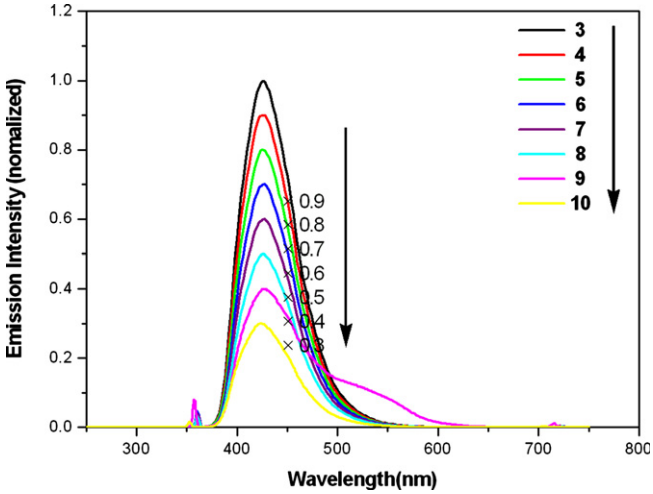

Fig. 2. Emission spectra of the hydrosilylated adducts (**3**–**10**) in THF with normalized intensity (the arrow in spectra indicates the order of number of the compounds).

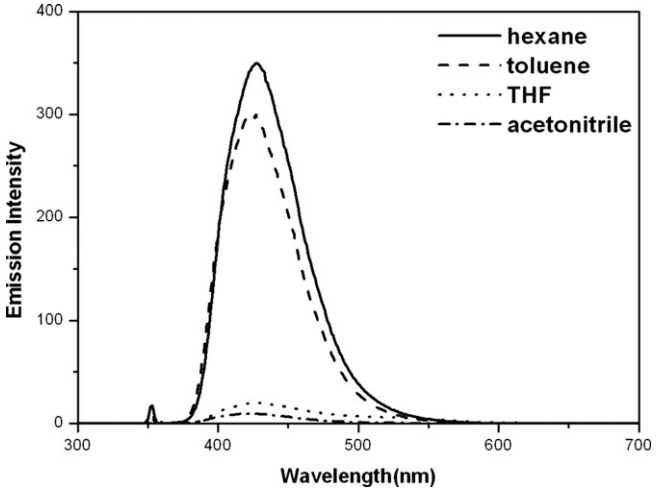

Fig. 3. Fluorescence spectra of **9** (10^{-5} M, λ_{ex} = 352 nm) in hexane (solid line), toluene (dashed line), THF (dotted line), and CH_3CN (dashed-dotted line).

with the emission spectra of the hydrosilylated adducts (**3**–**8** and **10**), the adduct **9** shows dual fluorescence with a shoulder band (533 nm) in the low energy region. The emission spectra of **9** in different solvents are shown in Fig. 3. The quantum yields of the emission of **9** were solvent dependent (Table 3). It is interesting to note that a charge transfer band was observed at around 533 nm when the measurement was taken in THF. These results suggest that the energy transfer [9,14] might readily take place in an efficient manner between the dimethylaminostyryl group (electron donor) and the dithienosilole moiety (acceptor) in **9**. The optical band gap energy of **2**–**10** were calculated from absorption edge of the UV–Vis absorption spectra. In the case of compound **9**, the UV-absorption appeared at slightly lower energy than those of the other hydrosilylated adducts leading to smaller optical band gap. Recently, TMS-DTS (Chart 1) as dithienosilole derivatives with low-lying LUMO levels has been reported to be useful as electron-transporting material in EL devices [10]. The PL quantum yields (Φ_F) of **2** and hydrosilylated adducts (**3**–**10**) were observed numerically over 80% compared with 9,10-diphenylanthracene.

The cyclic voltammograms (CVs) of some of the hydrosilylated adducts were measured in acetonitrile solution containing 0.1 M $LiClO_4$. The adduct **9** was measured in THF containing Bu_4NClO_4. Most of the compounds revealed that one oxidation peak appeared at about 1.0 V vs. SCE. The first oxidation peaks of the hydrosilylated adducts (**2**,**4**, **6**, **8** and **9**) appear at slightly lower potentials than that of TMS-DTS [5], indicating the slightly higher HOMOs of the

Table 3
Quantum yields[a] of **9** in different solvents

Compound	Hexane	Toluene	THF	CH_3CN
9	0.80	0.71	0.14	0.02

[a] Quantum yield was obtained using 9,10-diphenylanthracene as reference (Φ_F = 0.90).

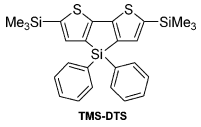

Chart 1.

Table 2
Optical and electrochemical properties of the hydrosilylated adducts (**3**–**10**)

Compound	λ_{max} (nm) (ε)[a]		Φ_F[b]	E_{ox}({E_{onset}}^{ox})[c]	HOMO/LUMO (eV)	λ_{ae}[e] (nm)	E_g[f] (eV)
	Absorption	Emission	sol	V vs. SCE			
3	356 (12192)	426	0.86	–	–	396	3.13
4	357 (14278)	428	0.84	0.98 (0.83)	−5.23/−2.10	396	3.13
5	357 (12072)	426	0.82	–	–	396	3.13
6	357 (15368)	428	0.80	0.99 (0.82)	−5.22/−2.11	396	3.13
7	358 (26352)	428	0.81	–	–	397	3.12
8	357 (15786)	426	0.85	0.93 (0.81)	−5.21/−2.07	395	3.14
9	362 (7465)	429, 533(sh)	0.17	0.59 (0.46)[d]	−4.99/−1.94	407	3.05
10	357 (20407)	424	0.40	–	–	397	3.13
Reactant (**2**)	354 (39075)	423	0.94	1.09 (0.82)	−5.22/−2.11	396	3.13
TMS-DTS[g]	356 (10220)	425	0.84	1.22	–	394	3.14

[a] Measured in 10^{-5} M THF solution, excited at the λ_{max} of absorption.
[b] Determined at 298 K in THF against 9,10-diphenylanthracene in THF as the standard (Φ_F = 0.90).
[c] Peak potential measured on a 4 mM solution in acetonitrile containing 100 mM of $LiClO_4$ using GC and Pt plate as working and counter electrodes at a scan rate of 20 mV/s.
[d] In THF containing 100 mM of Bu_4NClO_4 using Pt–Pt as the working electrodes and Ag^+/Ag as the reference.
[e] Absorption edge.
[f] Optical band gap taken from the absorption spectra.
[g] 2,6-Bis(trimethylsilyl)-4,4-diphenyldithieno[3,2-*b*:2',3'-*d*]silole [Ref. [5]].

hydrosilylated dithienosilole derivatives in accordance with the results of the calculated HOMO energy levels. Cyclic voltammetry was employed to evaluate the ionization potential (i.e., hole-injection ability) [7b]. The lower oxidation potentials (i.e., higher HOMO level) of the hydrosilylated adducts (**2**, **4**, **6**, **8** and **9**) might be expected a better hole-injection ability than that of TMS-DTS. The adduct **9** exhibited particularly the lower oxidation potential indicating the higher HOMO level of **9**, compared to that of the adducts (**2**, **4**, **6** and **8**). The HOMO energy levels of the adducts (**2**, **4**, **6**, **8** and **9**) are calculated from the onset of oxidation potential according to the equation, IP(ionization potential) = $\{(E_{onset})^{ox} + 4.4\}$V [11], and the LUMO energy level was obtained by the subtraction of optical band gap from the IP (Table 2).

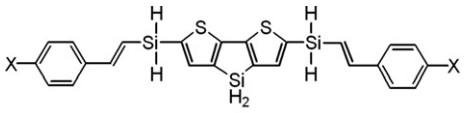

Scheme 2.

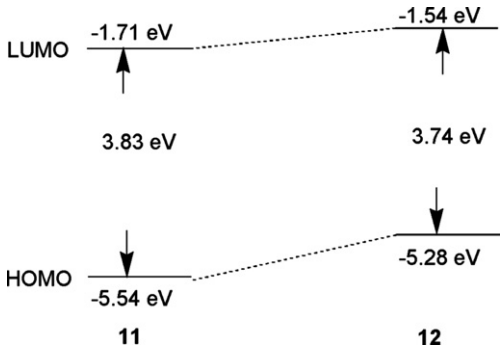

Fig. 4. Relative HOMO and LUMO energy levels of model compounds **11** and **12** derived from MO calculations at the level of B3LYP/6-31G(d,p).

2.3. Theoretical calculation on model compounds

We carried out theoretical calculations on the simplified model compound **11** and **12** (Scheme 2) at the level of B3LYP/6-31G(d,p) to learn more about the electronic structures.

The relative energy levels for model compounds are depicted in Fig. 4. As can be seen in Fig. 4, the HOMO–LUMO energy gap of **12** was calculated to be smaller relative to that of **11**. These results are in good agreement with the optical data of the compounds, i.e., slightly red-shifted UV absorption maxima for DTS derivatives (**9**) with dimethylaminostyryl group relative to that for the adduct (**6**) with styryl group. The non-bonding electrons on the nitrogen atom of auxochrome were involved in π-conjugation, partially. It was noted that both the HOMO and LUMO energy levels of **12** were increased by introduction of amino group on the both phenyl substituents. However, the HOMO of **12** was primarily affected by the amino group, as compared with the LUMO of **12**, leading to smaller HOMO–LUMO energy gap for **12** than that of **11**. Introduction of a powerful electron-donating group would tend to lower the HOMO–LUMO energy gap of **12**. Fig. 5 depicts the HOMO and LUMO profiles obtained from the calculations, showing the intramolecular charge-transfer transition [14] from highest occupied molecular orbital (HOMO) delocalized over the aminostyryl and DTS units through the $SiMe_2$ spacer in amino-derivative (**12**) to the lowest unoccupied molecular orbital (LUMO) mainly localized on the DTS unit.

3. Conclusion

In summary, we have synthesized eight novel 2,6-bis(ethenylsilyl)-4,4-diphenyldithienosilole derivatives (**3–10**) containing silylene-spacer via hydrosilylation in the presence of platinum catalyst. All hydrosilylations proceeded regio- and stereoselectively to give solely β-(*E*)-adducts (**3**–**10**). The UV–Vis absorption and emission bands were not affected by the R substituents on silicon atoms, which are connected to the dithienosilole ring. This phenomenon was possibly due to the interruption of π-conjugation by the silylene moiety simply serve as an insulating spacer. However, the emission spectra of the adduct **9** especially showed a band in the

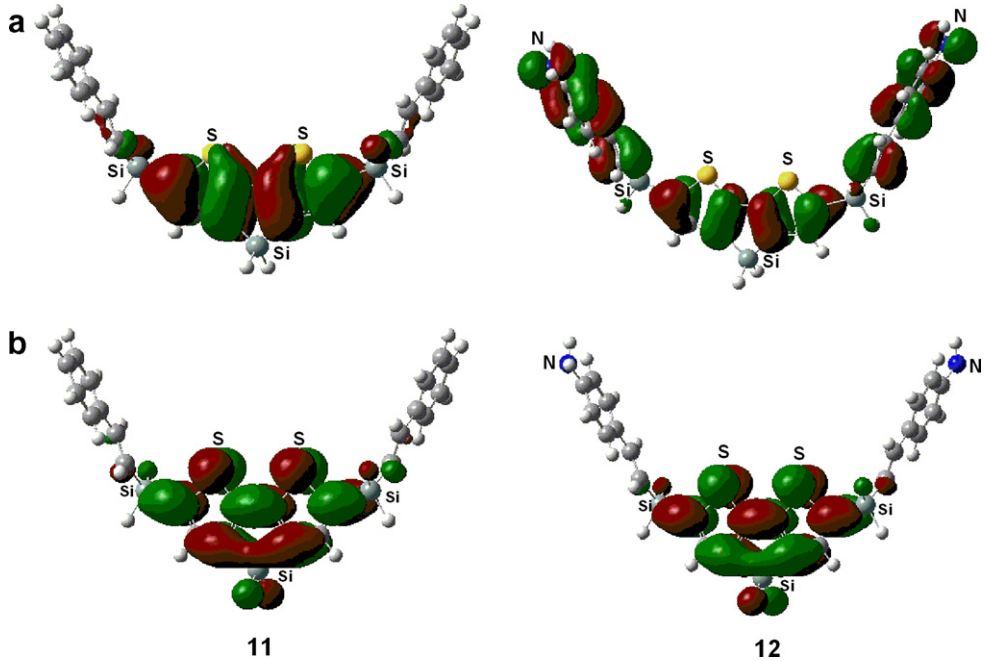

Fig. 5. (a) HOMO and (b) LUMO profiles for model compunds **11** and **12**, derived from MO calculations.

low-energy region, which are due to the energy transfer might take place in an efficient manner between the dimethylaminostyryl group (electron donor) and the dithienosilole moiety (acceptor) in **9**. These optical data are in good agreement with the results of theoretical calculations of the model compounds. The HOMO and LUMO profiles of model compounds showed the orbital interaction between the aminostyryl and DTS units through the $SiMe_2$ spacer in amino-derivative (**12**). The hydrosilylated adducts exhibited intense fluorescence emission and high quantum yields.

4. Experimental

4.1. General procedure

All platinum-catalyzed hydrosilylation reactions were carried out under an atmosphere of nitrogen. Yields of products **2**–**10** were calculated on the basis of the isolated products. The progress of the reaction was checked by TLC. ^1H, ^{13}C and ^{29}Si NMR spectra were recorded on Bruker Avance 400 and Varian 500 spectrometers in chloroform-*d* ($CDCl_3$) at 298 K. Chemical shifts were given as δ values referenced in parts per million (ppm) from tetramethylsilane (TMS) as internal standard. Silicon chemical shifts are referenced to the signal of TMS. Pure adducts **2**–**10** were separated by column chromatography using silica gel. Mass spectra were measured on a Shimadzu QP5000 instrument. UV–Vis absorption spectra were measured on JASCO V-530 spectrometer. The fluorescence spectra were obtained by a JASCO FP-6500 spectrofluorometer. The fluorescence quantum yields (Φ_F) were determined in argon-saturated solutions at 298 K in chloroform against 9,10-diphenylanthracene (Aldrich) in THF ($\Phi_F = 0.90$) as the standard. Elemental analysis was measured on a FISONE, EA1106. Melting points were measured with a Laboratory Devices-MEL-TEMP II apparatus.

4.2. Materials

Tetrahydrofuran (THF) and diethylether used as solvents were dried over sodium/benzophenone under a nitrogen atmosphere and distilled before use. *n*-Butyllithium (2.5 M in *n*-hexane), chlorodimethylsilane, *N*,*N*,*N*′,*N*′-tetramethylethylenediamine (TMEDA), phenylacetylene, 4-ethynyltoluene, *tert*-butylacetylene, trimethylsilylacetylene, triethylsilylacetylene, 4-ethynyl-*N*,*N*-dimethylaniline, 4-ethynylbenzonitrile, ethylenebis(triphenylphophine)-platinum(0), bis(divinyltetramethyldisiloxane)platinum(0) were obtained from Aldrich Chemical Co. and used without further purification. 2,6-Dibromo-4,4-diphenyldithienosilole (**1**) [5] and triphenylsilylacetylene [12] were prepared according to procedures reported in the literature.

4.3. Preparation of 2,6-bis(dimethylsilyl)-4,4-diphenyldithienosilole (**2**)

To a solution of 2,6-dibromo-4,4-diphenyldithienosilole (**1**) [5] (0.50 g, 0.99 mmol) in ether (30 mL) at −78 °C was added dropwise TMEDA (0.60 mL, 3.9 mmol) and *n*-butyllithium (2.5 M solution in hexane) (1.6 mL, 3.9 mmol). The mixture was stirred at −78 °C for 30 min, and warmed to room temperature. After the mixture was stirred for 1 h, chlorodimethylsilane (0.40 mL, 3.9 mmol) was added to the mixture at −78 °C. The resulting mixture was allowed to warm to room temperature and was stirred for 12 h. The mixture was hydrolyzed with water. The aqueous solution was extracted with ether and the organic layer was dried over $MgSO_4$. The solvent was evaporated by rotary evaporator. The resulting mixture was purified by column chromatography (silica gel, hexane) and reprecipitated from ethanol to give **2** (0.32 g, 0.69 mmol, 70% yield) as sparkling light yellow solids: m.p. 121–122; UV ($\lambda_{max,}$ in THF) 354 nm ($\varepsilon = 39075\ M^{-1}\ cm^{-1}$); emission ($\lambda_{max,}$ in THF) 423 nm; ^1H NMR (400 MHz, in $CDCl_3$) δ 0.41 (d, 12H, $SiMe_2$), 4.58 (sept, 2H, SiH), 7.34–7.48 (m, 8H, phenyl and thienylene protons), 7.62–7.65 (m, 4H, phenyl protons); ^{13}C NMR (400 MHz, in $CDCl_3$) δ −2.69, 128.15, 130.26, 131.92, 135.40, 137.70, 138.50, 142.12, 155.98; ^{29}Si NMR (500 MHz, in $CDCl_3$) δ −23.58, −4.44; MS: *m*/*z* 462 (M^+). Anal. Calc. for $C_{24}H_{26}S_2Si_3$: C, 62.28; H, 5.66. Found: C, 62.24; H, 5.85%.

4.4. Hydrosilylation of tert-butylacetylene with **2**

To a mixture of ethylenebis(triphenylphophine)platinum(0) (1.0 mol%), 2,6-bis(dimethylsilyl)-4,4-diphenyldithienosilole (**2**) (0.50 g, 1.1 mmol) in 10 mL of hexane added *tert*-butylacetylene (0.20 g, 2.2 mmol). After the resulting mixture was stirred at 40 °C for 12 h and then hydrolyzed with water. The aqueous solution was extracted with ether and the organic layer was dried over $MgSO_4$. The solvent was evaporated by rotary evaporator. The resulting mixture was chromatographed on a silica gel column with hexane as eluent to afford hydrosilylated adduct **3** (0.59 g, 0.97 mmol, 88% yield) as a white solids: m.p. 126–127 °C; UV ($\lambda_{max,}$ in THF) 356 nm ($\varepsilon = 12192\ M^{-1}\ cm^{-1}$); emission ($\lambda_{max,}$ in THF) 426 nm; ^1H NMR (400 MHz, in $CDCl_3$) δ 0.38 (s, 12H, $SiMe_2$), 1.02 (s, 18H, CMe_3), 5.66 (d, 2H, $J = 19.2$ Hz, vinylic protons), 6.18 (d, 2H, $J = 19.2$ Hz, vinylic protons), 7.28 (s, 2H, bithienylene protons), 7.34–7.42 (m, 6H, phenyl protons), 7.63–7.66 (m, 4H, phenyl protons); ^{13}C NMR (400 MHz, in $CDCl_3$) δ −1.05, 28.96, 35.23, 120.22, 128.06, 130.11, 132.35, 135.45, 136.95, 141.35, 141.64, 155.90, 159.92; ^{29}Si NMR (500 MHz, in $CDCl_3$) δ −22.03, −14.42. Anal. Calc. for $C_{36}H_{46}S_2Si_3$: C, 68.95; H, 7.39. Found: C, 68.74; H, 7.61%.

Compounds **4**–**10** were prepared as described for **3**, by using trimethylsilylacetylene, triethylsilylacetylene, phenylacetylene, tolylacetylene, triphenylsilylacetylene, 4-ethynyl-*N*,*N*-dimethylaniline, or 4-ethynylbenzonitrile, respectively. The compounds **4**, **5** and **8** were prepared by using bis(divinyltetramethyldisiloxane)platinum(0) instead of ethylenebis(triphenyl-phosphine)platinum(0). Data for **4**: light ivory solids (yield 51%); m.p. 144–145 °C; UV ($\lambda_{max,}$ in THF) 357 nm ($\varepsilon = 14278\ M^{-1}\ cm^{-1}$); Emission ($\lambda_{max,}$ in THF) 428 nm; ^1H NMR (400 MHz, in $CDCl_3$) δ 0.08 (s, 18H, $SiMe_3$), 0.39 (s, 12H, $SiMe_2$), 6.68 (d, 2H, $J = 22.6$ Hz, vinylic protons), 6.76 (d, 2H, $J = 22.1$ Hz, vinylic protons), 7.29 (s, 2H, bithienylene protons), 7.32–7.46 (m, 6H, phenyl protons), 7.63–7.66 (m, 4H, phenyl protons); ^{13}C NMR (400 MHz, in $CDCl_3$) δ −1.92, −0.39, 128.11, 132.04, 135.42, 135.77, 137.19, 140.42, 141.79, 147.43, 153.48, 156.00; ^{29}Si NMR (500 MHz, in $CDCl_3$) δ −21.93, −15.62, −7.15. Anal. Calc. for $C_{34}H_{46}S_2Si_5$: C, 61.94; H, 7.03. Found: C, 61.80; H, 7.06%. Data for **5**: white solids (yield 50%); m.p. 94–96 °C. UV ($\lambda_{max,}$ in THF) 357 nm ($\varepsilon = 12072\ M^{-1}\ cm^{-1}$); emission ($\lambda_{max,}$ in THF) 426 nm; ^1H NMR (400 MHz, in $CDCl_3$) δ 0.39 (s, 12H, $SiMe_2$), 0.59 (q, 12H, $J = 8.04$, 15.82 Hz, $SiCH_2CH_3$), 0.94 (t, 18H, $J = 8.04$ Hz, CH_3CH_2Si), 6.68 (d, 2H, $J = 20.6$ Hz, vinylic protons), 6.74 (d, 2H, $J = 20.6$ Hz, vinylic protons), 7.30 (s, 2H, bithienylene protons), 7.33–7.41 (m, 6H, phenyl protons), 7.62–7.65 (m, 4H, phenyl protons); ^{13}C NMR (400 MHz, in $CDCl_3$) δ −1.59, 3.12, 7.37, 128.09, 130.15, 132.30, 135.43, 137.21, 140.53, 141.74, 149.34, 149.99, 155.98; ^{29}Si NMR (500 MHz, in $CDCl_3$) δ −22.05, −15.78, −1.02. Anal. Calc. for $C_{40}H_{58}S_2Si_5$: C, 64.62; H, 7.86. Found: C, 64.43; H, 8.27%. Data for **6**: yellow solids (yield 63%): m.p. 135–136 °C; UV ($\lambda_{max,}$ in THF) 357 nm ($\varepsilon = 15368\ M^{-1}\ cm^{-1}$); emission ($\lambda_{max,}$ in THF) 428 nm; ^1H NMR (300 MHz, in $CDCl_3$) δ 0.47 (s, 12H, $SiMe_2$), 6.56 (d, 2H, $J = 18.9$ Hz, vinylic protons), 6.97 (d, 2H, $J = 18.9$ Hz, vinylic protons), 7.26–7.45 (m, 18H, phenyl and thienylene protons), 7.59–7.64 (m, 4H, phenyl protons); ^{13}C NMR (400 MHz, in $CDCl_3$) δ −1.21, 126.53, 126.62, 128.13, 128.33, 128.55, 130.21, 132.11, 135.49, 137.38, 137.95, 140.31, 142.01, 145.60, 156.05;

^{29}Si NMR (500 MHz, in $CDCl_3$): δ −22.05, −13.86; MS: *m/z* 666 (M^+). Anal. Calc. for $C_{40}H_{38}S_2Si_3$: C, 72.02; H, 5.74. Found: C, 71.67; H, 5.88%. Data for **7**: white solids (yield 63%): m.p. 126–128 °C; UV ($\lambda_{max,}$ in THF) 358 nm (ε = 26 352 M^{-1} cm^{-1}); emission ($\lambda_{max,}$ in THF) 428 nm; ^{1}H NMR (400 MHz, in $CDCl_3$) δ 0.48 (s, 12H, $SiMe_2$), 2.31 (s, 6H, methyl protons), 6.52 (d, 2H, *J* = 19.1 Hz, vinylic protons), 6.96 (d, 2H, *J* = 19.1 Hz, vinylic protons), 7.14 (d, 4H, *J* = 8 Hz, phenylene protons), 7.34–7.43 (m, 12H, phenyl, phenylene and thienylene protons), 7.62–7.65 (m, 4H, phenyl protons); ^{13}C NMR (400 MHz, in $CDCl_3$) δ −1.17, 21.26, 125.13, 126.54, 128.12, 129.25, 130.18, 132.17, 135.30, 135.49, 137.32, 138.26, 140.49, 141.95, 145.51, 156.03; ^{29}Si NMR (500 MHz, in $CDCl_3$) δ −22.06, −13.92; MS: *m/z* 694 (M^+). Anal. Calc. for $C_{42}H_{42}S_2Si_3$: C, 72.56; H, 6.09. Found: C, 72.64; H, 6.21%. Data for **8**: white solids (yield 37%): m.p. 82–83 °C; UV ($\lambda_{max,}$ in THF) 357 nm (ε = 15 786 M^{-1} cm^{-1}); emission ($\lambda_{max,}$ in THF) 426 nm; ^{1}H NMR (400 MHz, in $CDCl_3$) δ 0.44 (s, 12H, $SiMe_2$), 6.92 (d, 2H, *J* = 22.1 Hz, vinylic protons), 7.26 (d, 2H, *J* = 22.1 Hz, vinylic protons), 7.30 (s, 2H, bithienylene protons), 7.32–7.44 (m, 24H, phenyl protons), 7.50 (dd, 12H, *J* = 1.52, 7.50 Hz, phenyl protons), 7.61–7.67 (m, 4H, phenyl protons); ^{13}C NMR (400 MHz, in $CDCl_3$) δ −1.67, 127.87, 128.02, 128.12, 129.54, 130.08, 134.12, 135.42, 135.49, 136.00, 137.39, 139.92, 141.92, 146.27, 154.31; ^{29}Si NMR (500 MHz, in $CDCl_3$) δ −22.11, −17.16, −15.02. Anal. Calc. for $C_{64}H_{58}S_2Si_5$: C, 74.51; H, 5.67. Found: C, 74.80; H, 5.94%.

Compound **9** was prepared using the same procedure as that described for **3** except 4-ethynyl-*N*,*N*-dimethylaniline was used instead of *tert*-butylacetylene for 24 h. Pure **9** was isolated by chromatography (eluent: hexane/THF = 10/1) in 38% yield (white solids). Data for **9**: m.p. 156–157 °C. UV (λ_{max}, in THF) 362 nm (ε = 7465 M^{-1} cm^{-1}); emission (λ_{max}, in THF) 429 and 533 (sh) nm; ^{1}H NMR (400 MHz, in $CDCl_3$) δ 0.46 (s, 12H, $SiMe_2$), 2.95 (s, 12H, $N(CH_3)_2$), 6.31 (d, 2H, *J* = 19.0 Hz, vinylic protons), 6.66 (d, 4H, *J* = 9.0 Hz, phenylene protons), 6.91 (d, 2H, *J* = 19.0 Hz, vinylic protons), 7.33–7.40 (m, 12H, phenyl, phenylene and thienylene protons), 7.64 (m, 4H, phenyl protons); ^{13}C NMR (400 MHz, in $CDCl_3$) δ 1.00, 40.53, 109.38, 112.38, 127.12, 128.18, 130.21, 130.32, 131.76, 135.40, 136.57, 137.28, 141.03, 142.42, 150.23, 155.85; ^{29}Si NMR (500 MHz, in $CDCl_3$) δ −22.09, −14.06. Anal. Calc. for $C_{44}H_{48}N_2S_2Si_3$: C, 70.15; H, 6.42; N, 3.72. Found: C, 69.78; H, 6.63; N, 3.83%.

Compound **10** was isolated by chromatography (eluent: hexane/THF = 15/1) in 34% yield (light yellow solids). Data for **10**: m.p. 125–127 °C; UV (λ_{max}, in THF) 357 nm (ε = 20 407 M^{-1} cm^{-1}); emission (λ_{max}, in THF) 424 nm; ^{1}H NMR (400 MHz, in $CDCl_3$) δ 0.51 (s, 12H, $SiMe_2$), 6.73 (d, 2H, *J* = 19.1 Hz, vinylic protons), 6.96 (d, 2H, *J* = 19.1 Hz, vinylic protons), 7.35–7.38 (m, 8H, phenyl and thienylene protons), 7.51 (d, 4H, *J* = 8.04 Hz, phenylene protons), 7.60–7.64 (m, 8H, phenyl and phenylene protons); ^{13}C NMR (400 MHz, in $CDCl_3$) δ −1.47, 111.44, 118.89, 127.07, 127.69, 128.18, 130.36, 131.87, 132.42, 135.46, 137.61, 139.38, 142.04, 142.30, 143.50, 156.10; ^{29}Si NMR (500 MHz, in $CDCl_3$) δ −22.69, −13.52. Anal. Calc. for $C_{42}H_{36}N_2S_2Si_3$: C, 70.34; H, 5.06. Found: C, 70.61; H, 5.43%.

4.5. CV measurements

CV measurements were carried out using a three-electrode system in an acetonitrile solution containing 100 mM of $LiClO_4$ as the supporting electrolyte and 4 mM of the substrate. Glassy carbon and Pt plate were used as the working and Pt wire counter electrodes, and SCE was used as the reference electrode. In case of **9**, CV was measured in THF solution containing 100 mM of Bu_4NClO_4 using Pt–Pt as the working electrodes and Ag^+/Ag as the reference. The current–voltage curve was recorded at room temperature on a Hokuto Denko HAB-151 potentiostat/galvanostat.

4.6. Molecular orbital caculations on **11** and **12**

The density functional theory (DFT) calculations were carried out using the GAUSSIAN 03 program package [13]. The Becke-three-parameter-Lee–Yang–Parr hybrid functional was employed with the 6-31G(d,p) basis set. Simplified models are used, in which all substituents on the silicon and nitrogen atoms are replaced by hydrogen atoms.

Acknowledgments

The work has been supported by Regional Industrial Engineering Development Foundation Grant (10027347-2006-01).

References

[1] (a) L.H. Sommer, E.W. Pietrusza, F.C. Whitmore, J. Am. Chem. Soc. 69 (1947) 188;
(b) I. Ojima, in: S. Patai, Z. Rappoport (Eds.), The Chemistry of Organic Silicon Compounds, John Wiley & Sons Ltd, New York, 1989;
(c) R.-M. Chen, K.-M. Chien, K.-T. Wong, B.-Y. Jin, T.-Y. Luh, J. Am. Chem. Soc. 119 (1997) 11321–11322;
(d) A. Mori, E. Takahisa, H. Kajiro, K. Hirabayashi, Y. Nishihara, T. Hiyama, Chem. Lett. (1998) 443–444;
(e) E. Lukevics, O. Pudova, R. Sturkovich, A. Gaukhman, J. Organomet. Chem. 346 (1998) 297–303;
(f) A. Mori, E. Takahisa, H. Kajiro, Y. Nishihara, Macromolecules 33 (2000) 1115–1116;
(g) E. Lukevics, V. Ryabova, P. Arsenyan, S. Belyakov, J. Popelis, O. Pudova, J. Organomet. Chem. 610 (2000) 8–15;
(h) S.E. Denmark, Z. Wang, Org. Lett. 7 (2001) 1073–1076;
(i) B. Marciniec, Silicon Chem. 1 (2002) 155–175;
(j) K. Itami, K. Mitsudo, A. Nishino, J.-I. Yoshida, J. Org. Chem. 67 (2002) 2645–2652;
(k) W. Wu, C.-J. Li, Chem. Commun. (2003) 1668–1669;
(l) T. Lee, I. Jung, K.H. Song, C. Baik, S. Kim, D. Kim, S.O. Kang, J. Ko, Organometallics 23 (2004) 4184–4191;
(m) H. Aneetha, W. Wu, J.G. Verkade, Organometallics 24 (2005) 2590–2596.
(2) J. Ohshita, A. Kunai, Acta Polym. 49 (1998) 379–403.
[3] (a) J. Ohshita, A. Takata, H. Kai, A. Kunai, K. Komaguchi, M. Shiotani, A. Adachi, K. Sakamaki, K. Okita, Y. Harima, Y. Kunugi, K. Yamashita, M. Ishikawa, Organometallics 19 (2000) 4492–4498;
(b) J. Ohshita, S. Kangai, Y. Tada, H. Yoshida, K. Sakamaki, A. Kunai, Y. Kunugi, J. Organomet. Chem. 692 (2007) 1020–1024.
[4] (a) J. Ohshita, T. Hamaguchi, E. Toyoda, A. Kunai, K. Komaguchi, M. Shiotani, Organometallics 18 (1999) 1717–1723;
(b) J. Ohshita, T. Sumida, A. Kunai, Macromolecules 33 (2000) 8890–8893;
(c) J. Ohshita, M. Nodono, A. Takata, H. Kai, A. Adachi, K. Sakamaki, K. Okita, A. Kunai, Macromol. Chem. Phys. 201 (2000) 851–857.
(5) J. Ohshita, M. Nodono, H. Kai, T. Watanabe, A. Kunai, K. Komaguchi, M. Shiotani, A. Adachi, K. Okita, Y. Harima, K. Yamashita, M. Ishikawa, Organometallics 18 (1999) 1453–1459.
[6] (a) S. Yamaguchi, K. Tamao, Bull. Chem. Soc. Jpn. 69 (1996) 2327–2334;
(b) S. Yamaguchi, K. Tamao, J. Chem. Soc., Dalton Trans. 22 (1998) 3693–3702;
(c) S. Yamaguchi, R.-Z. Jin, K. Tamao, J. Am. Chem. Soc. 121 (1999) 2937–2938;
(d) S. Yamaguchi, R.-Z. Jin, Y. Itami, K. Tamao, J. Am. Chem. Soc. 121 (1999) 10420–10421;
(e) S. Yamaguchi, T. Goto, K. Tamao, Angew. Chem., Int. Ed. 39 (2000) 1695–1697.
[7] (a) S. Kyushin, M. Ikarugi, M. Goto, H. Hiratsuka, H. Matsumoto, Organometallics 15 (1996) 1067–1070;
(b) T. Lee, K.H. Song, I. Jung, Y. Kang, S.-H. Lee, S.O. Kang, J. Ko, J. Organomet. Chem. 691 (2006) 1887–1896.
(8) S. Yamaguchi, K. Tamao, Chem. Lett. 34 (2005) 2–7.
[9] (a) Y.-J. Cheng, T.-Y. Luh, Chem. Eur. J. 10 (2004) 5361–5368;
(b) Y.-J. Cheng, S. Basu, S.-J. Luo, T.-Y. Luh, Macromolecules 38 (2005) 1442–1446;
(c) Y.-J. Cheng, T.-Y. Luh, Macromolecules 38 (2005) 4563–4568;
(d) Y.-J. Cheng, T.-Y. Luh, Chem. Commun. (2006) 4669–4678;
(e) H.-W. Wang, M.-Y. Yeh, C.-H. Chen, T.-S. Lim, W. Fann, T.-Y. Luh, Macromolecules 41 (2008) 2762–2770.
[10] (a) A. Adachi, J. Ohshita, A. Kunai, J. Kido, K. Okita, Chem. Lett. (1998) 1233–1234;
(b) A. Adachi, J. Ohshita, A. Kunai, K. Okita, Jpn. J. Appl. Phys. 38 (1999) 2148–2149.
(11) A.K. Agrawal, S.A. Jenekhe, Chem. Mater. 8 (1996) 579–589.
(12) A. Naka, M. Ishikawa, J. Organomet. Chem. 611 (2000) 248–255.
(13) M.J. Frisch, G.W. Trucks, H.B. Schlegel, G.E. Scuseria, M.A. Robb, J.R. Cheeseman, J.A. Montgomery, Jr., T. Vreven, K.N. Kudin, J.C. Burant, J.M. Millam, S.S. Iyengar, J. Tomasi, V. Barone, B. Mennucci, M. Cossi, G. Scalmani, N. Rega, G.A.

Petersson, H. Nakatsuji, M. Hada, M. Ehara, K. Toyota, R. Fukuda, J. Hasegawa, M. Ishida, T. Nakajima, Y. Honda, O. Kitao, H. Nakai, M. Klene, X. Li, J.E. Knox, H.P. Hratchian, J.B. Cross, V. Bakken, C. Adamo, J. Jaramillo, R. Gomperts, R.E. Stratmann, O. Yazyev, A.J. Austin, R. Cammi, C. Pomelli, J.W. Ochterski, P.Y. Ayala, K. Morokuma, G.A. Voth, P. Salvador, J.J. Dannenberg, V.G. Zakrzewski, S. Dapprich, A.D. Daniels, M.C. Strain, O. Farkas, D.K. Malick, A.D. Rabuck, K. Raghavachari, J.B. Foresman, J.V. Ortiz, Q. Cui, A.G. Baboul, S. Clifford, J. Cioslowski, B.B. Stefanov, G. Liu, A. Liashenko, P. Piskorz, I. Komaromi, R.L. Martin, D.J. Fox, T. Keith, M.A. Al-Laham, C.Y. Peng, A. Nanayakkara, M. Challacombe, P.M.W. Gill, B. Johnson, W. Chen, M.W. Wong, C. Gonzalez, J.A. Pople, GAUSSIAN 03, Gaussian, Inc., Wallingford, CT, 2003.

[14] (a) C. Moreau, F. Serein-Spirau, J.-F. Létard, R. Lapouyade, G. Jonusauskas, C. Rullière, J. Phys. Chem. B 102 (1998) 1487–1497;
(b) G. Kwak, T. Masuda, Macromolecules 35 (2002) 4138–4142;
(c) Z.R. Grabowski, K. Rotkiewcz, W. Rettig, Chem. Rev. 103 (2003) 3899–4032;
(d) C.-H. Zhao, A. Wakamiya, Y. Inukai, S. Yamaguchi, J. Am. Chem. Soc. 128 (2006) 15934–15935;
(e) A. Wakamiya, K. Mori, S. Yamaguchi, Angew. Chem., Int. Ed. 46 (2007) 4273–4276.